Tuning Surface States of Metal/Polymer Contacts Toward Highly Insulating Polymer-Based Dielectrics

Yifei Wang, Shamima Nasreen, Deepak Kamal, Zongze Li, Chao Wu, Jindong Huo, Lihua Chen, Rampi Ramprasad, and Yang Cao*

Cite This: https://doi.org/10.1021/acsami.1c12854
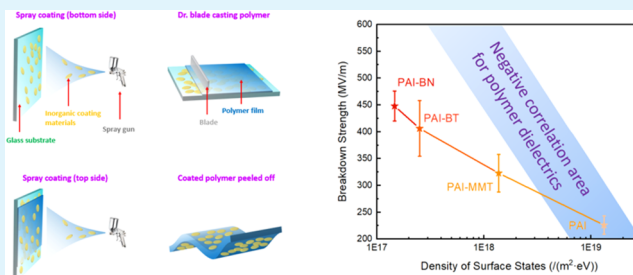
Read Online

ACCESS | Metrics & More | Article Recommendations | Supporting Information

ABSTRACT: Metal–polymer interface plays a crucial role in controlling the dielectric performance in all flexible electronics. Ideally, the formation of the Schottky barrier due to the large band offset of the electron affinity of the polymer over the work function of the electrode should sufficiently impede the charge injection. Arguably, however, such an injection barrier has hardly been indisputably verified in polymer–metal junctions due to the ever-existing surface states, which dramatically compromise the barrier thus leading to undesired high electrical conduction. Here, we demonstrate experimentally a clear negative correlation between the breakdown strength and the density of surface states in polymer dielectrics. The existence of surface states reduces the effective barrier height for charge injection, as further revealed by density functional theory calculations and photoinjection current measurements. Based on these findings, we present a surface engineering method to enhance the breakdown strength with the application of nanocoatings on polymer films to eliminate surface states. The density of surface states is reduced by 2 orders of magnitude when the polymer is coated with a layer of two-dimensional hexagonal boron nitride nanosheets, leading to about 100% enhancement of breakdown strength. This work reveals the critical role played by surface states on electrical breakdown and provides a versatile surface engineering strategy to curtail surface states, broadly applicable for all polymer dielectrics.

KEYWORDS: polymer–metal interface, surface states, breakdown strength, nanocoatings, 2D materials

1. INTRODUCTION

With recent explosive developments in electrifications of transportations, renewable power, and defense industries, there are great needs of electrostatic systems with advanced energy storage and high-payload conversion efficiencies.[1−3] To achieve high-energy densities in dielectric capacitors, dielectric materials are required to sustain ever-increasing applied electric fields.[4] Polymers are the most promising materials for energy storage applications due to their high breakdown strength, low loss, lightweight, flexibility, and scalability, which have stimulated great efforts to improve their insulating capabilities, including both the molecular and composite (nano)structural engineering.[5−7] With the identification of promising high-performance polymer-based dielectric alternatives to existing materials, it becomes urgent to advance the understanding of the mechanisms of high-field aging and electrical breakdown to translate these new materials toward practical use. However, owing to the complex interplays of multiple governing factors for high-field phenomena in polymer dielectrics, the study of their electrical breakdown mechanism remains only at the stage of phenomenological explanations.

The research path toward highly insulating polymer dielectrics begins with adjusting their bulk electrical properties by molecular design.[8,9] For example, favorable electrical insulating properties can be realized by the introduction of rigid segments to suppress charge hopping or tunneling. Wu et al. designed an all-organic polymer dielectric polyoxafluoronorbornene, which possesses a nonconjugated polymer backbone that could restrict intrachain and interchain charge mobility.[10] The emergence of polymer composites, especially nanofillers contained in thin films, provides a golden opportunity to tailor the properties of the polymer matrix.[11−14] Besides, as the relationship between properties and structures can be reflected more intuitively in composite materials, some theoretical assumptions of electrical breakdown could be verified experimentally. For example, it is believed that breakdown paths would be elongated when local defects with accumulated charges are introduced into the polymer matrix, which are partially proved when higher breakdown strengths
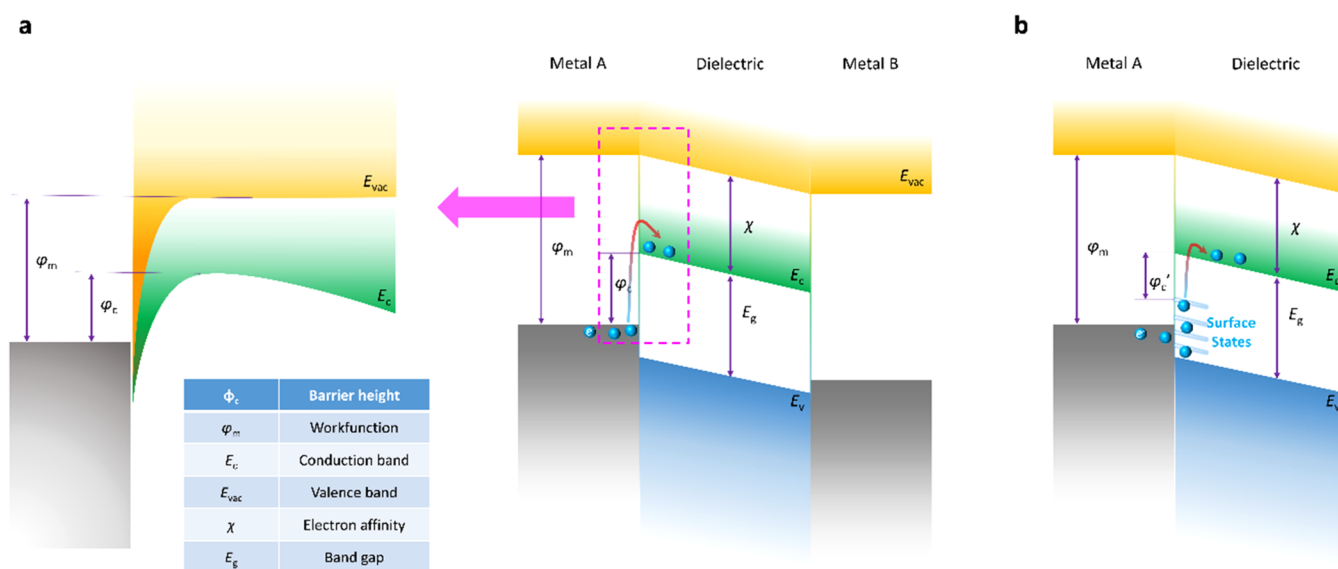
Figure 1. Schematic illustration. (a) Band structure of a metal–polymer contact and (b) that with considering surface states.
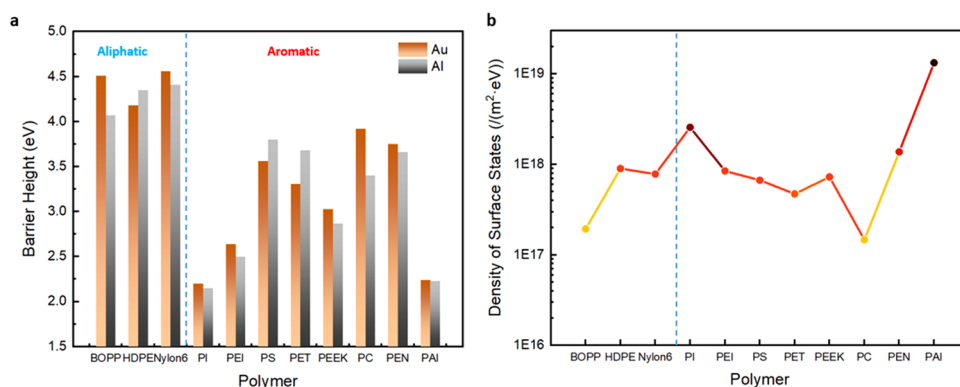

Figure 2. Barrier heights and densities of surface states of polymer–metal contacts. (a) Barrier heights with gold and aluminum electrodes, respectively, and (b) densities of surface states of polymer dielectrics.

are observed in polymer composites containing minute amount of dielectric inorganic nanoparticles (<3 vol %).[15] Electrical conduction of polymers depends not only on the bulk but also interfaces that decide how charges are injected into polymer dielectrics from electrodes.[16] The first clue comes from comparisons among sandwich-structured composites that show significantly enhanced breakdown strengths by just moving more insulating layers from the inside to the outside.[17,18] It has been further confirmed in surface-modified polymer films with inorganic coatings, which can deliver favorable electrical insulating capabilities even under high-temperature working conditions.[19−22] These encouraging results manifest how important the surface is when polymers are subjected to high voltage. However, present-day efforts to control or exploit surfaces are restricted to trial-and-error approaches.

The charge injection barrier height is theoretically defined as the difference between the work function of the metal electrode and the electron affinity of the dielectric polymer.[23] A typical energy-band diagram of an ideal metal–polymer heterostructure is illustrated in Figure 1a, where the band structure near the interface is highlighted, showing the Schottky effect.[24] In principle, for a specific polymer, the barrier height is associated with the work function of the metal

electrode. For example, if the electrode metal is replaced from gold to aluminum, the change in the barrier height could ideally be the same as the difference of the work function between gold and aluminum. However, the experimental barrier height is almost independent of the metal electrode work function. The surface defects, believed as one satisfactory explanation, which exist in all polymers and even other solid dielectrics, will introduce defect energy levels between the conduction and valence bands. When in contact with metal electrodes, these surface states will facilitate, under bias voltages, the charge carriers' injection from the electrode, which then leap to the conduction band of the dielectric polymer, as shown in Figure 1b. This multistage transition alleviates the leap difficulty of electrons and significantly reduces the barrier height (φ_c'). For instance, a practical Schottky-barrier height of merely ∼1 eV for Au–polyethylene interfaces, rather than the theoretically expected 4.5 eV.[25]

In this work, we revealed for the first time a universal law in polymer dielectrics that demonstrates a negative correlation between breakdown strengths and densities of surface states. Polymers with lower densities of surface states are inclined to be more electrical insulating, based on a data set of carefully studied 11 polymer films that include both aliphatic and aromatic polymers (molecular structures are shown in Figure
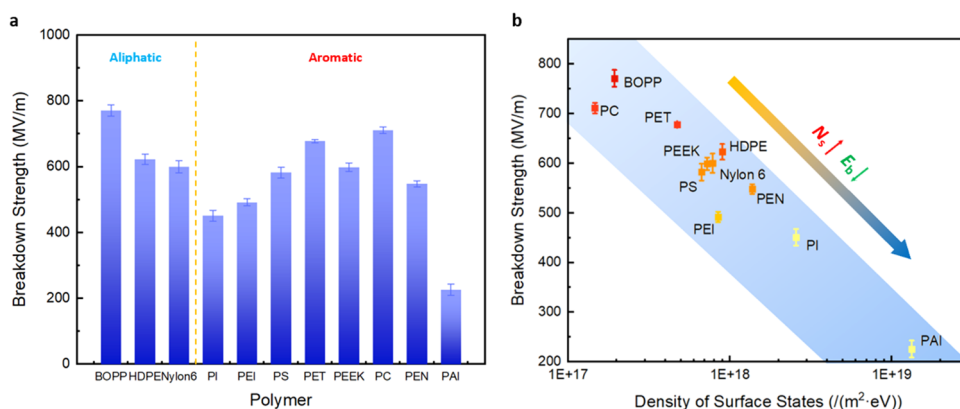
Figure 3. Relationship between the breakdown strength and density of surface states in polymers. (a) Breakdown strengths and (b) their relationship with densities of surface states of polymer dielectrics.

S1). Moreover, leveraging upon this finding, we tailored the surface states of a lab-fabricated polyamideimide film by the utilization of nanocoatings (boron nitride, barium titanate, montmorillonite). Highly enhanced breakdown strengths (100% improvement), accompanied by low densities of surface states (2 orders of magnitude suppressed), are observed in the sample with optimized coating materials, which revealed not only the important role of surface states with respect to the underlying physical mechanisms of dielectric breakdown but also a pathway for developing/enhancing high-performance dielectric polymers via surface engineering, a facial approach readily applicable to commercial and lab emerging polymer dielectrics.

2. RESULTS AND DISCUSSION

2.1. Barrier Heights and Surface States. Barrier heights are derived by the photoinjection current (J_p) produced by shining a monochromatized light beam with a particular wavelength on a metal−polymer−metal contact and then collected by a biasing circuit (experimental setup and incident beam spectrum are shown in Figures S2 and S3). Figures S4 and S5 show the spectrum of photoinjection current as a function of incident light wavelength. By extracting the data of the right ridge of J_p peak, barrier heights of all samples are summarized in Figure 2a. Compared with aromatic polymers, aliphatic polymers show relatively higher barrier heights, implying their high electrical insulating capabilities for dielectric applications. For example, BOPP, which possesses the highest barrier heights among all tested films, is the benchmark material in polymer capacitors. A more interesting finding is that using a gold electrode cannot ensure an absolutely higher barrier height, although it has a higher work function than aluminum. This erratic variation of barrier heights reflects the contribution of surface states to some extent.

Assuming surface states are uniformly distributed in the forbidden gap, the density of surface states can be estimated as

$$N_s = \frac{\varepsilon_i \varepsilon_0}{dq} \left| \frac{(\varphi_{m1} - \varphi_{m2}) - (\varphi_{c1} - \varphi_{c2})}{\varphi_{c1} - \varphi_{c2}} \right| \quad (1)$$

where ε_i is the dielectric constant of the interfacial layer, d is its thickness, ε_0 is vacuum permittivity, and q is the charge of an electron. φ_{m1} and φ_{m2} are the work functions of gold (5.38 eV) and aluminum (4.17 eV), respectively.[26] The thickness of the

interfacial layer d is of the order of the interatomic spacing and the dielectric constant ε_i of such a thin layer can be approximated by the free space value.[27] Here, we assume d = 5 Å and ε_i = 1. The threshold of photoinjections, i.e., barrier heights, φ_{c1} and φ_{c2} are obtained in the samples with different metal electrodes. N_s of all of the polymers are summarized in Figure 2b. Polycarbonate (PC), which is recognized as a pervasive packaging and connecting material in electronic and electrical industries, possesses the lowest N_s among all of the tested polymers, meaning its favorable electrical insulating properties may mainly stem from the low-defects surface. On the contrary, some promising candidates for high-temperature dielectric energy storage, such as polyetherimide (PEI), polyether-ether-ketone (PEEK), and polyethylene naphthalate (PEN), have higher N_s, which happens that all of these polymers are reported to have high dielectric loss, especially under high voltage/temperature. The surface effects on the electrical insulating properties of polymers are gradually unveiled depending on these scenarios.

2.2. Breakdown Strengths and Their Relationship with the Densities of Surface States. The insulating capability of a dielectric material can be directly reflected by its breakdown strength. Here, the breakdown strengths of polymers are analyzed by a two-parameter Weibull statistic

$$P(E) = 1 - \exp((-E/E_b)^\beta) \quad (2)$$

where $P(E)$ is the cumulative probability of electrical failure, E is the experimental breakdown strength, E_b is the characteristic breakdown strength for which there is 63.2% probability of sample failure, and β evaluates the scattering of data.[28] More than 10 samples went through the DC breakdown test for each kind of polymers, and their E_b are summarized in Figure 3a. Notably, aliphatic polymers present relatively higher breakdown strength than aromatic polymers, such as BOPP, whose distinguished insulating characteristics endow itself as the definitive candidate for dielectric polymer capacitors.[29]

After a comprehensive analysis by synthetically considering the surface states and dielectric breakdown of all polymers, a heartening result has been dug out that a negative correlation exists between N_s and E_b, which means it is highly possible to achieve high E_b in a polymer with less surface states, as shown in Figure 3b. For example, an impressive breakdown strength of 770 MV m^{-1} can be observed in BOPP, which is 40% higher than that in PEN, owing to the N_s of the former is 1 order of magnitude lower than that of the latter. Moreover, a dark
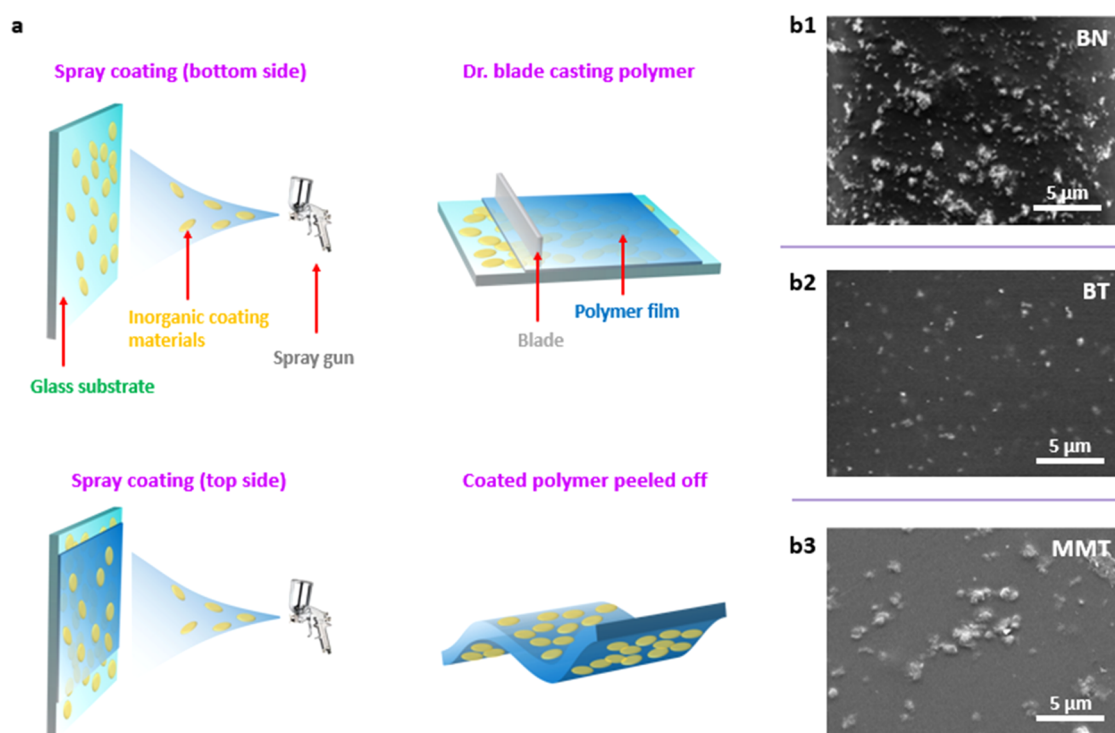
C

Figure 4. Coated polymers' preparation. (a) Schematic illustration of manufacturing coated polymer samples. (b) SEM of coated polymers with different coating materials (top view).
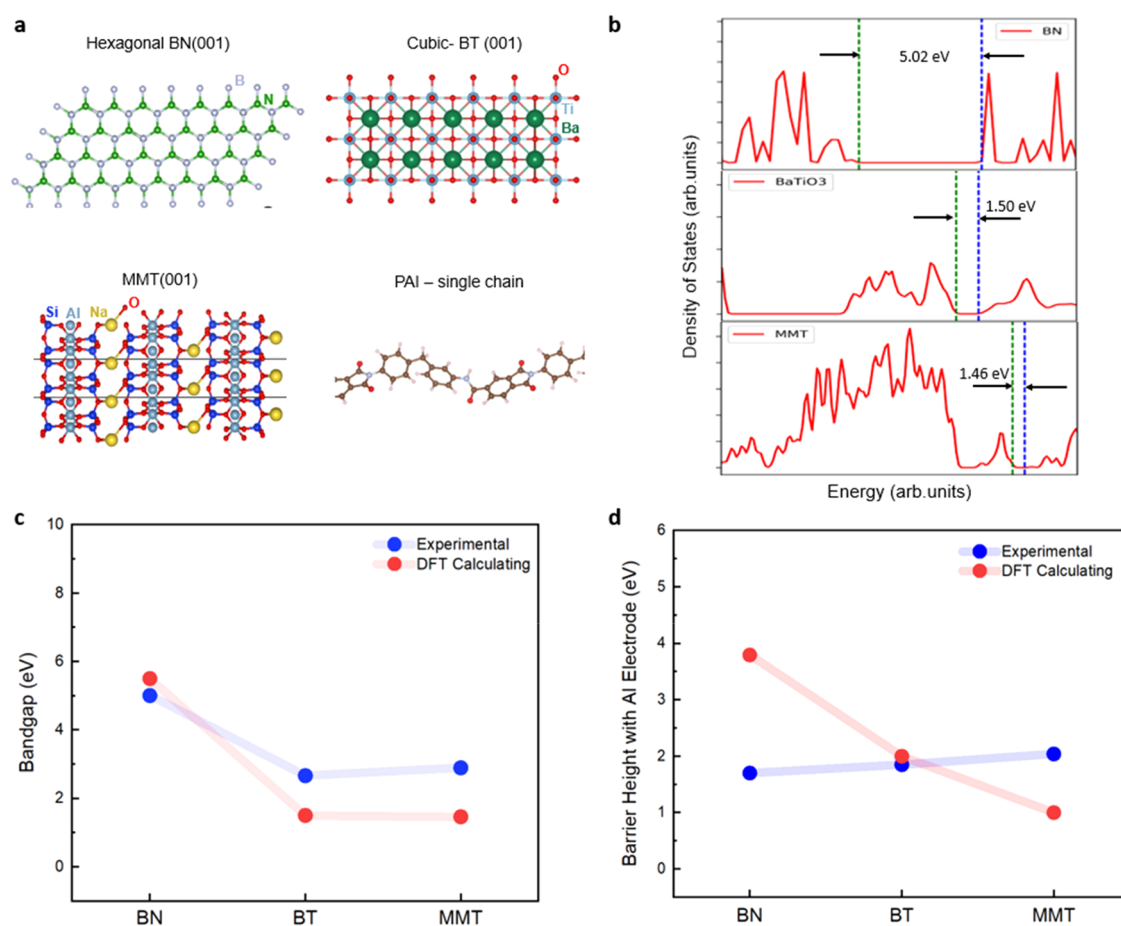

Figure 5. DFT calculated results. (a) Molecular structure and (b) calculated density of states of BN, BT, and MMT. Comparison between calculated and experimental results of the (c) band gaps of BN, BT, and MMT and (d) their barrier heights with aluminum electrodes.
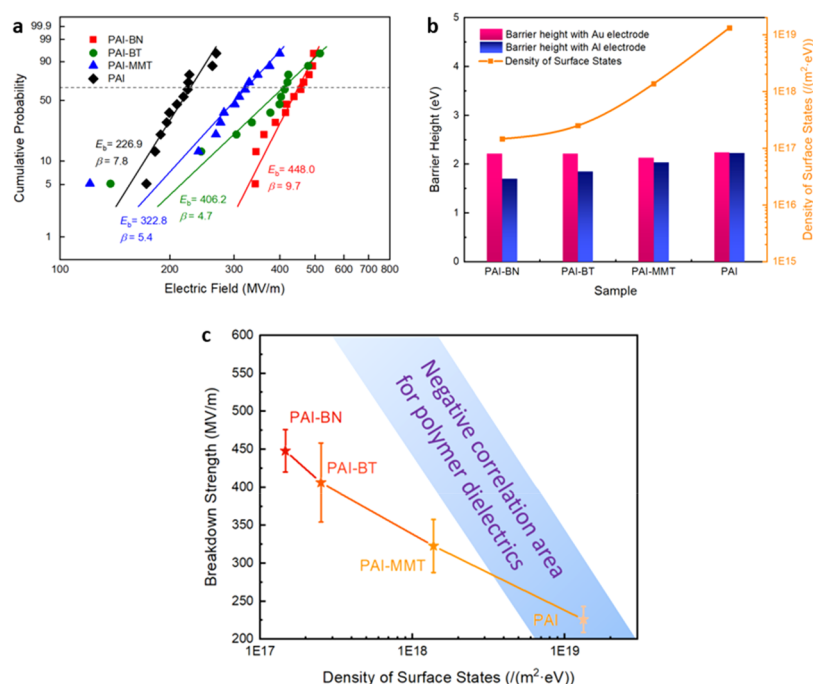
D

Figure 6. Relationship between the breakdown strength and density of surface states of coated polymers. (a) Weibull distribution of breakdown strengths. (b) Barrier heights with gold and aluminum electrodes, respectively, and density of surface states of PAI films with different coating materials. (c) Relationship between the breakdown strength and density of surface states of the coated PAI.

region is marked in Figure 3b artificially, where all of the data points lie inside. This half-quantitative analysis result implies that the upper limit of the breakdown strength of a polymer has already been decided when it possesses a certain kind of surface states. Inferentially, to break this bottle neck, it will be unavoidable but also effective to eliminate the surface defects as well as N_s by surface manipulation.

2.3. Tuning Surface States and Improving Breakdown Strengths. The inverse correlation between E_b and N_s portends a promising method to improve the E_b of polymers by suppressing their surface states. To testify this hypothesis and further apply it to materials modification, we coated three different kinds of inorganic nanopowders on polyamideimide (PAI) films, respectively, to adjust their surface states as well as E_b, and the manufacturing process is illustrated in Figure 4a. For coating materials, barium titanate nanoparticle (BTNP) is the most epidemic lead-free high-k dielectric, boron nitride nanosheet (BNNS) has an extremely high band gap showing favorable electrical insulating capability, and montmorillonite nanosheet (MMTNS) has been well known by its anisotropic electrically conductive properties. Owing to their unique dielectric and electrical characteristics, they are recognized as epidemic fillers for constructing high-performance dielectric nanocomposites.[30−32] Figure 4b shows the surface morphology of coated polymers. A little aggregation can be observed in a large-scale area with homogeneous distribution of coating materials, which may introduce surface states and act as a weakness for breakdown ignition.

Density functional theory (DFT) calculations are utilized here to inspect the density of states and electronic band structures of the three coating materials. Compared with BT nanoparticles with cubic phase, BN and MMT possess layered molecular structures (Figure 5a), potentially showing anisotropic properties. If we assume that BN and MMT nanosheets are perfectly aligned on the polymer surface during the gravity-

driven spraying coating process, the overall density of states can be computed using DFT (Figure 5b). As an insulating material, it could be seen that no energy states exist in a wide range of energy level in BN, whose band gap is 5.02 eV. In contrast, the band gap of BT, recognized as a high-k dielectric, is much smaller and insensitive to crystal direction due to the symmetric crystal phase of cubic BT. The most attractive feature of MMT is its anisotropic conductivity, being relatively conductive along in-plane but insulating through thickness direction. As evidenced in Figure 5b, a band gap of 1.46 eV can be seen, which is comparable with that of BT. To verify computations, we performed UV−vis spectrum band gap (Figure S7) measurements. A comparison between the computed and observed values of band gap is made in Figure 5c, which ascertains the accuracy of the simulations employed.

Further, electron injection barriers between coating materials and Al electrodes were computed using DFT, assuming no direct interfacial contact.[33] The computed barrier heights are summarized in Figure 5d. As expected, BN coating can endow the largest barrier height due to its ultrahigh band gap, while the smallest barrier height was found in the case with MMT coating. However, when compared to the barrier heights of coated PAI films obtained with different coating materials by photocurrent measurements (Figures S8 and S9, with aluminum electrodes), there is a large discrepancy between DFT and experimental barrier heights. For example, a completely reversed relation of barrier heights among those three coatings can be found in Figure 5d, where PAI with BNNS coatings shows the lowest experimental barrier height. The E_b of the three coated polymer films were analyzed by Weibull distribution and summarized in Figure 6a. Although highly insulating BN coating shows the lowest barrier height with an aluminum electrode, it endows PAI with the highest E_b among all coated samples, which is about 40% higher than for MMTNSs. These observations suggest that the barrier height

may not be the only factor that could decide the charge injection as well as E_b, and the surface states should be taken into account.[27] A noteworthy factor is that the weight content of inorganic part in the whole film is only 1%, indicating that surfaces must be playing a significant role. In comparison, the E_b of inorganic/polymer nanocomposites can hardly be adjusted more than 20%, by just introducing nanofillers into the polymer matrix with the same content.[34,35]

We deduced the value of densities of states based on the barrier heights of coated PAI films with different electrodes (gold and aluminum, Figures S8 and S9), where a clear negative correlation between E_b and N_s of coated polymers is found, which shows similar trends with that in pure polymers, as shown in Figure 6c, where the dark area denotes the location of the polymers data point (extended based on the dark region in Figure 3b). For instance, the N_s of PAI-MMT is an order of magnitude higher than that of PAI-BN. This proposes and demonstrates a novel and effective method to improve E_b by choosing optimized coating materials to lower the N_s of dielectric polymers. Meanwhile, it should not be ignored that the data points of the coated PAI is a little away from the dark region. As we introduced inorganic materials in coated polymers, they can no longer be regarded as pure polymers. That may be the reason that the negative relation between the breakdown strength and the density of surface states for the coated sample follows a different slope. It may be expected that the quantitative relationship between E_b and N_s applicable to all dielectrics could be further obtained, if those data of inorganic materials are measured and summarized in the same way. Then, this emerging theory can substantially guide the exploration of favorable dielectric materials based on not only surface modification but also composite design.

2.4. Discussion on the Negative Correlation between Breakdown Strengths and the Densities of Surface States. We find a negative correlation between breakdown strength (E_b) and density of surface state (N_s), and hereby highlight the governing effect of surface statement on the electrical insulating properties of dielectric polymers. Aliphatic polymers, including BOPP, most important polymer dielectrics for capacitors, possess fewer surface states, which is considered a major factor to ensure its long-time service reliability under high-voltage conditions. With the ever-increasing working temperature and voltage level, severe challenges for exploring high-temperature dielectric polymers have been raised. For example, a high voltage DC bus of 800 V has been reported recently for fast-charging electric vehicles (EVs). On the other hand, because of the low thermal limit of BOPP capacitors (only 85 °C), a cumbersome cooling system has to be used to lower the working temperature of the motor drives, while the new generation of wideband semiconductors can be readily operated at temperatures >150 °C for enhanced power density and pay-load efficiency.[36] Aromatic polymers, especially the family of polyimides (such as PI and PEI), are long considered as promising candidates for high-temperature energy storage and conversion due to their high glass-transition temperatures. However, it can be observed that their densities of surface states are 1 magnitude higher than that of BOPP. Such highly defective surface may lead not only to an inferior breakdown strength but also a high dielectric loss, which brings in a significant challenge for harsh condition electrifications.[19]

In the past decade, surface modification, especially via the application of inorganic coatings, has been regarded as an effective novel strategy to improve the breakdown strength and

inhibit dielectric loss of polymer dielectrics. In this study, we reveal for the first time that these encouraging improvements originate from the reduction of surface defect states. PAI films prepared in laboratory study are adopted as a model material system, for coating with BNNSs, BTNPs, and MMTNSs, respectively, to demonstrate the inverse correlation between E_b and N_s. PAI with BNNS coating shows the lowest N_s, which is 1 order of magnitude lower than for the MMTNSs-coated sample, giving rise to a remarkable enhancement in E_b of about 40%. In-depth analysis further indicates that the underlying mechanism of optimized coating for improved electrical insulating capability resides in the largely suppressed surface defect states N_s of dielectrics.

3. CONCLUSIONS

In summary, a negative correlation between E_b and N_s in polymer dielectrics is identified, and this hypothesis is confirmed and further applied by adjusting the surface states of polymers by coating different inorganic nanomaterials. The value of N_s is strongly related to the kind of coating materials; meanwhile, the coated polymer with the lowest N_s can deliver the highest E_b. These findings present a theoretical foundation of surface engineering and provide a guideline for creating high-performance polymer dielectrics with excellent electrical insulation.

4. METHODS

4.1. Materials. The PI film with a thickness of 8 μm was provided by DuPont (Kapton), PEI (5 μm) was purchased from SABIC, BOPP was provided by Bolore (7.5 μm), and PEEK (5 μm) was obtained from Victrex UK. PET (8 μm), PS (10 μm), and PC (10 μm), (PEN (12 μm), HDPE (8 μm), Nylon6 (16 μm)) were purchased from Goodfellow. Polyamideimide (PAI) resin solution was provided by Elantas Elatrical Insulation (Tritherm A981-H-25). For coating materials, BN, BT, and MMT were supplied by US Research Nanomaterials, Acros Organics, and BYK Additives Inc., respectively. N,N-dimethylformamide (DMF) was purchased from Fisher Chemical as the dilute solvent.

4.2. Coated Film Fabrication. A spray solution and a casting solution are used to make the coating layer and the polymer dielectric layer, respectively. The casting solution was prepared by diluting PAI resin into DMF, assisted by strong magnetic stirring. The thickness of the PAI film is 20 μm. To make coating precursor solutions, BN, BT, or MMT were first dispersed in DMF by tip-sonication, respectively, with a filler-solvent weight ratio of 1:250. Then, the PAI resin solution was added into the solution, followed by magnetic stirring for 24 h. The mixture was subjected to a 10 min sonication again just before spraying. To manufacture coated films, one layer of coating was sprayed on a glass substrate and dried under ambient conditions. Afterward, the casting solution was poured on the top of the coating layer and shaped by a doctor blade. After drying in an 80 °C oven for 10 min, a PAI thin film can be obtained, followed by spraying another coating layer on its topside. The film was further dried in a 130 °C oven for a whole night to completely evaporate all the solvent, and then cured at 300 °C under vacuum condition for imidization. Finally, the coated PAI films were peeled off from the glass substrate and subjected to characterization.

4.3. Characterization. The morphology and elemental analysis of nanocoatings were characterized with SEM and EDAX (FEI Teneo LVSEM) to locate coating materials. For photocurrent measurements, a 450-W xenon short-arc lamp was used as a light source, which was mounted in the Fluorolog-3 Horiba Scientific instrument with Horiba Jobin Yvon double grating monochromator. The wavelength range was chosen from 200 to 600 nm with 10 nm slit width and 0.1 nm increment. The polymer films are coated both sides by a 6002-8 Ted Pella, Inc. sputter coater for 90 s at 20 mA current for a ~100 nm

thick Au coating. Al coating was performed with the Denton Bench-Top Turbo (BTT) physical vapor deposition (PVD) process via resistive heating of metallic precursors. The polymer sample with metal coating was mounted in a designed sample holder facing a light source and connected to the DC regulated power supply. The other side of the coated film was connected to a Model 6514 Keithley electrometer to record the current. The whole setup was exposed to equilibration in an ambient atmosphere for 3−4 h until the residual current reached to a constant value. Then, a bias voltage of 100 V was applied in dark condition for 1 h. The measured photocurrent was recorded with an electrometer against the incident light in the entire wavelength range starting from a higher frequency. Electric breakdown tests were carried out with a linear voltage ramp of 300 V/s source generated by a resistor−capacitor (RC) circuit. The power supply can be shut off through an interlock input when the breakdown occurred, and the breakdown voltage was recorded with a peak-holding voltmeter. The breakdown strength can be deduced by dividing breakdown voltage by the thickness of polymer thin film.

4.4. Deducing Barrier Height From Photocurrent Spectrum. The J_p of a Schottky conduction in a metal-dielectric structure can be expressed to a first-order approximation when exposed under a given photon flux

$$J_p = AT^2 f(x) \tag{3}$$

where $x = (h\nu - \phi_c)/kT$, A is a constant, k is Boltzmann's constant, T is the absolute temperature, $h\nu$ is the incident photon energy, ϕ_c is the threshold energy, and

$$f(x) = \begin{cases} e^x - \dfrac{e^{2x}}{2^2} + \dfrac{e^{3x}}{3^3} - \dots & (x < 0) \\[2mm] \dfrac{\pi^2}{6} + \dfrac{x^2}{2} - \left(e^x - \dfrac{e^{2x}}{2^2} + \dfrac{e^{3x}}{3^3} - \dots \right) & (x > 0) \end{cases} \tag{4}$$

. Then, a familiar Fowler's relationship can be deduced

$$J_p \propto (h\nu - \varphi_c)^2 \tag{5}$$

when the x^2 term is the only significant part in $f(x)$ with a larger value of x.[26] Here, gold and aluminum, adopted as the electrode materials, are coated on 11 representative dielectric thin films to construct metal−polymer contacts, respectively.

4.5. DFT Calculations. In this work, we used the DFT formalism as implemented in Vienna Ab initio Simulation Package (VASP)[37] to do the density of states and band structure computations. Within this scheme, a plane-wave cutoff of 600 eV and a k-point density of 0.1 Å^{-1} were used. The Van der Waals dispersion interactions, which are important for describing interlayer interactions, were estimated with the nonlocal density functional vdWDF2.[38] Refitted Perdew-Wang 86, the exchange-correlation (XC) functional associated with vdWDF2, was adopted for the geometry optimization, for which convergence was assumed when the atomistic forces become less than 0.01 eV/Å.[39] Finally, to accurately compute electronic properties, such as conduction band minimum (CBM), the valence band maximum (VBM), and the band gap, HSE06-XC functional[40] was used. With this framework, VBM is the highest energy level of Kohn−sham equations, which is occupied by an electron, while CBM is the lowest energy level that is unoccupied. The band gap was then obtained from a DFT calculation by simply taking the difference between VBM and CBM.

To compute the barrier height (φ_c) using DFT, three properties are required. They are the maximum energy at which electrons reside in the metal or the metal Fermi level (E_F), the energy of the first vacant energy level in the polymer, which is CBM, and the interaction between Al and polymer which introduces an interface dipole moment (D) and shifts polymer CBM with respect to Al E_F by $\Delta\varphi = -eD/(2a)$.[41] Here, e is an electron charge and a is the area of the interface. Finally, the electron injection barrier is then determined using $\varphi_c = E_F - E_{CBM} + \Delta\varphi$. Recently, we established that this approach can be effectively simplified by ignoring $\Delta\varphi$ and considering

the polymer single-chain model.[33] This simplification allows us to decouple the computation into two parts where we independently determine the CBM of the polymer and the E_F of Al. So, the computation of φ_c finally boils down to the computation of the CBM of the polymer. This scheme is employed to perform high-throughout φ_c computations within this work.

■ ASSOCIATED CONTENT

ⓢ Supporting Information

The Supporting Information is available free of charge at https://pubs.acs.org/doi/10.1021/acsami.1c12854.

> Molecular structures of polymer dielectrics in this study, illustration of the photocurrent setup, incident light beam spectrum for photocurrent test, photocurrents and barrier heights of polymer dielectrics with gold electrode and aluminum electrodes, band gaps of 2D nanocoating materials, and photocurrents and barrier heights of coated polymer dielectrics of polymer dielectrics with gold and aluminum electrodes (PDF)

■ AUTHOR INFORMATION

Corresponding Author

Yang Cao − *Electrical Insulation Research Center, Institute of Materials Science, University of Connecticut, Storrs, Connecticut 06269, United States; Department of Electrical and Computer Engineering, University of Connecticut, Storrs, Connecticut 06269, United States;* ⓞ orcid.org/0000-0001-7034-2792; Email: yang.cao@uconn.edu

Authors

Yifei Wang − *Electrical Insulation Research Center, Institute of Materials Science, University of Connecticut, Storrs, Connecticut 06269, United States;* ⓞ orcid.org/0000-0002-0848-9977

Shamima Nasreen − *Electrical Insulation Research Center, Institute of Materials Science, University of Connecticut, Storrs, Connecticut 06269, United States;* ⓞ orcid.org/0000-0002-1504-8555

Deepak Kamal − *School of Materials Science and Engineering, Georgia Institute of Technology, Atlanta, Georgia 30332, United States;* ⓞ orcid.org/0000-0003-1943-7774

Zongze Li − *Electrical Insulation Research Center, Institute of Materials Science, University of Connecticut, Storrs, Connecticut 06269, United States; Department of Electrical and Computer Engineering, University of Connecticut, Storrs, Connecticut 06269, United States*

Chao Wu − *Electrical Insulation Research Center, Institute of Materials Science, University of Connecticut, Storrs, Connecticut 06269, United States;* ⓞ orcid.org/0000-0002-4565-8231

Jindong Huo − *Electrical Insulation Research Center, Institute of Materials Science, University of Connecticut, Storrs, Connecticut 06269, United States*

Lihua Chen − *School of Materials Science and Engineering, Georgia Institute of Technology, Atlanta, Georgia 30332, United States;* ⓞ orcid.org/0000-0002-9852-8211

Rampi Ramprasad − *School of Materials Science and Engineering, Georgia Institute of Technology, Atlanta, Georgia 30332, United States;* ⓞ orcid.org/0000-0003-4630-1565

Complete contact information is available at:
https://pubs.acs.org/10.1021/acsami.1c12854

Author Contributions

Y.C., Y.W., and S.N. devised the original concept. Y.W. was responsible for materials' preparation. Y.W. and S.N. performed photocurrent measurements. D.K., L.C., and R.R. carried out simulation studies. Y.W., Z.L., and C.W. measured breakdown strengths. Y.C., Y.W., S.N., Z.L., C.W., and J.H. analyzed the data. Y.C., Y.W., and S.N. wrote the first draft of the manuscript, and all authors participated in manuscript revision.

Notes

The authors declare no competing financial interest.

■ REFERENCES

(1) Karden, E.; Ploumen, S.; Fricke, B.; Miller, T.; Snyder, K. Energy Storage Devices for Future Hybrid Electric Vehicles. *J. Power Sources* **2007**, *168*, 2−11.

(2) Cao, Y.; Irwin, P. C.; Younsi, K. The Future of Nanodielectrics in The Electrical Power Industry. *IEEE Trans. Dielectr. Electr. Insul.* **2004**, *11*, 797−807.

(3) Tan, D. Q. Review of Polymer-Based Nanodielectric Exploration and Film Scale-Up for Advanced Capacitors. *Adv. Funct. Mater.* **2020**, *30*, No. 1808567.

(4) Chen, Q.; Shen, Y.; Zhang, S.; Zhang, Q. M. Polymer-Based Dielectrics with High Energy Storage Density. *Annu. Rev. Mater. Res.* **2015**, *45*, 433−458.

(5) Chu, B.; Zhou, X.; Ren, K.; Neese, B.; Lin, M.; Wang, Q.; Bauer, F.; Zhang, Q. M. A Dielectric Polymer with High Electric Energy Density and Fast Discharge Speed. *Science* **2006**, *313*, 334−336.

(6) Li, H.; Gadinski, M. R.; Huang, Y.; Ren, L.; Zhou, Y.; Ai, D.; Han, Z.; Yao, B.; Wang, Q. Crosslinked Fluoropolymers Exhibiting Superior High-Temperature Energy Density and Charge−Discharge Efficiency. *Energy Environ. Sci.* **2020**, *13*, 1279−1286.

(7) Chen, J.; Wang, Y.; Dong, J.; Chen, W.; Wang, H. Ultrahigh Energy Storage Density at Low Operating Field Strength Achieved in Multicomponent Polymer Dielectrics with Hierarchical Structure. *Compos. Sci. Technol.* **2021**, *201*, No. 108557.

(8) Zhang, Z.; Wang, D. H.; Litt, M. H.; Tan, L. S.; Zhu, L. High-Temperature and High-Energy-Density Dipolar Glass Polymers Based on Sulfonylated Poly(2,6-dimethyl-1,4-phenylene oxide). *Angew. Chem., Int. Ed.* **2018**, *57*, 1528−1531.

(9) Wu, C.; Deshmukh, A. A.; Li, Z.; Chen, L.; Alamri, A.; Wang, Y.; Ramprasad, R.; Sotzing, G. A.; Cao, Y. Flexible Temperature-Invariant Polymer Dielectrics with Large Bandgap. *Adv. Mater.* **2020**, *32*, No. 2000499.

(10) Li, Z.; Treich, G. M.; Tefferi, M.; Wu, C.; Nasreen, S.; Scheirey, S. K.; Ramprasad, R.; Sotzing, G. A.; Cao, Y. High Energy Density and High Efficiency All-Organic Polymers with Enhanced Dipolar Polarization. *J. Mater. Chem. A* **2019**, *7*, 15026−15030.

(11) Pan, Z.; Yao, L.; Zhai, J.; Yao, X.; Chen, H. Interfacial Coupling Effect in Organic/Inorganic Nanocomposites with High Energy Density. *Adv. Mater.* **2018**, *30*, No. 1705662.

(12) Dang, Z. M.; Yuan, J. K.; Yao, S. H.; Liao, R. J. Flexible Nanodielectric Materials with High Permittivity for Power Energy Storage. *Adv. Mater.* **2013**, *25*, 6334−6365.

(13) Lin, Y.; Sun, C.; Zhan, S.; Zhang, Y.; Yuan, Q. Ultrahigh Discharge Efficiency and High Energy Density in Sandwich Structure $K_{0.5}Na_{0.5}NbO_3$ Nanofibers/Poly(vinylidene fluoride) Composites. *Adv. Mater. Interfaces* **2020**, *7*, No. 2000033.

(14) Luo, H.; Zhou, X.; Ellingford, C.; Zhang, Y.; Chen, S.; Zhou, K.; Zhang, D.; Bowen, C. R.; Wan, C. Interface Design for High Energy Density Polymer Nanocomposites. *Chem. Soc. Rev.* **2019**, *48*, 4424−4465.

(15) Wang, Y.; Cui, J.; Yuan, Q.; Niu, Y.; Bai, Y.; Wang, H. Significantly Enhanced Breakdown Strength and Energy Density in Sandwich-Structured Barium Titanate/Poly(vinylidene fluoride) Nanocomposites. *Adv. Mater.* **2015**, *27*, 6658−6663.

(16) Khanchaitit, P.; Han, K.; Gadinski, M. R.; Li, Q.; Wang, Q. Ferroelectric Polymer Networks with High Energy Density and Improved Discharged Efficiency for Dielectric Energy Storage. *Nat. Commun.* **2013**, *4*, No. 2845.

(17) Li, Q.; Liu, F.; Yang, T.; Gadinski, M. R.; Zhang, G.; Chen, L. Q.; Wang, Q. Sandwich-Structured Polymer Nanocomposites with High Energy Density and Great Charge-Discharge Efficiency at Elevated Temperatures. *Proc. Natl. Acad. Sci. U.S.A.* **2016**, *113*, 9995−10000.

(18) Liu, F.; Li, Q.; Cui, J.; Li, Z.; Yang, G.; Liu, Y.; Dong, L.; Xiong, C.; Wang, H.; Wang, Q. High-Energy-Density Dielectric Polymer Nanocomposites with Trilayered Architecture. *Adv. Funct. Mater.* **2017**, *27*, No. 1606292.

(19) Azizi, A.; Gadinski, M. R.; Li, Q.; AlSaud, M. A.; Wang, J.; Wang, Y.; Wang, B.; Liu, F.; Chen, L. Q.; Alem, N.; Wang, Q. High-Performance Polymers Sandwiched with Chemical Vapor Deposited Hexagonal Boron Nitrides as Scalable High-Temperature Dielectric Materials. *Adv. Mater.* **2017**, *29*, No. 1701864.

(20) Zhou, Y.; Li, Q.; Dang, B.; Yang, Y.; Shao, T.; Li, H.; Hu, J.; Zeng, R.; He, J.; Wang, Q. A Scalable, High-Throughput, and Environmentally Benign Approach to Polymer Dielectrics Exhibiting Significantly Improved Capacitive Performance at High Temperatures. *Adv. Mater.* **2018**, *30*, No. 1805672.

(21) Wang, Y.; Li, Z.; Wu, C.; Cao, Y. High-Temperature Dielectric Polymer Nanocomposites with Interposed Montmorillonite Nanosheets. *Chem. Eng. J.* **2020**, *401*, No. 126093.

(22) Wu, X.; Tang, S.; Song, G.; Zhang, Z.; Tan, D. Q. High-Temperature Resistant Polypropylene Films Enhanced by Atomic Layer Deposition. *Nano Express* **2021**, *2*, No. 010025.

(23) Zhou, P.; Wang, Y.; Nasreen, S.; Cao, Y. Barrier Heights of Polymer-Electrode Interfaces Measured via Photo Injection Current Method. *Surf. Interfaces* **2021**, *24*, No. 101070.

(24) Rikken, G. L. J. A.; Braun, D.; Staring, E. G. J.; Demandt, R. Schottky Effect at A Metal-Polymer Interface. *Appl. Phys. Lett.* **1994**, *65*, 219−221.

(25) Coelho, R. *Physics of Dielectrics for the Engineer*; Elsevier, 2012; Vol. *1*, p 136.

(26) Mizutani, T.; Takai, Y.; Osawa, T.; Ieda, M. Barrier Heights and Surface States of Metal-Polymer (PET) Contacts. *J. Phys. D: Appl. Phys.* **1976**, *9*, 2253.

(27) Cowley, A.; Sze, S. Surface states and barrier height of metal-semiconductor systems. *J. Appl. Phys.* **1965**, *36*, 3212−3220.

(28) Wang, Y.; Li, Y.; Wang, L.; Yuan, Q.; Chen, J.; Niu, Y.; Xu, X.; Wang, Q.; Wang, H. Gradient-Layered Polymer Nanocomposites with Significantly Improved Insulation Performance for Dielectric Energy Storage. *Energy Storage Mater.* **2020**, *24*, 626−634.

(29) Rabuffi, M.; Picci, G. Status Quo And Future Prospects for Metallized Polypropylene Energy Storage Capacitors. *IEEE Trans. Plasma Sci.* **2002**, *30*, 1939−1942.

(30) Li, Q.; Chen, L.; Gadinski, M. R.; Zhang, S.; Zhang, G.; Li, U.; Iagodkine, E.; Haque, A.; Chen, L. Q.; Jackson, N.; Wang, Q. Flexible High-Temperature Dielectric Materials from Polymer Nanocomposites. *Nature* **2015**, *523*, 576−579.

(31) Zhu, Y.; Zhu, Y.; Huang, X.; Chen, J.; Li, Q.; He, J.; Jiang, P. High Energy Density Polymer Dielectrics Interlayered by Assembled Boron Nitride Nanosheets. *Adv. Energy Mater.* **2019**, *9*, No. 1901826.

(32) Ding, F.; Liu, J.; Zeng, S.; Xia, Y.; Wells, K. M.; Nieh, M. P.; Sun, L. Biomimetic Nanocoatings with Exceptional Mechanical, Barrier, And Flame-Retardant Properties from Large-Scale One-Step Coassembly. *Sci. Adv.* **2017**, *3*, No. e1701212.

(33) Kamal, D.; Wang, Y.; Tran, H. D.; Chen, L.; Li, Z.; Wu, C.; Nasreen, S.; Cao, Y.; Ramprasad, R. Computable Bulk and Interfacial

Electronic Structure Features as Proxies for Dielectric Breakdown of Polymers. *ACS Appl. Mater. Interfaces* **2020**, *12*, 37182−37187.

(34) Zhang, X.; Shen, Y.; Xu, B.; Zhang, Q.; Gu, L.; Jiang, J.; Ma, J.; Lin, Y.; Nan, C. W. Giant Energy Density and Improved Discharge Efficiency of Solution-Processed Polymer Nanocomposites for Dielectric Energy Storage. *Adv. Mater.* **2016**, *28*, 2055−2061.

(35) Hao, Y.; Wang, X.; Bi, K.; Zhang, J.; Huang, Y.; Wu, L.; Zhao, P.; Xu, K.; Lei, M.; Li, L. Significantly Enhanced Energy Storage Performance Promoted by Ultimate Sized Ferroelectric BaTiO$_3$ Fillers In Nanocomposite Films. *Nano Energy* **2017**, *31*, 49−56.

(36) Aghabali, I.; Bauman, J.; Emadi, A. In *Analysis of Auxiliary Power Unit and Charging for an 800 V Electric Vehicle*, IEEE Transportation Electrification Conference and Expo (ITEC), 2019; pp 1−6.

(37) Kresse, G.; Furthmüller, J. Efficiency of Ab-Initio Total Energy Calculations for Metals and Semiconductors Using A Plane-Wave Basis Set. *Comput. Mater. Sci.* **1996**, *6*, 15−50.

(38) Lee, K.; Murray, É. D.; Kong, L.; Lundqvist, B. I.; Langreth, D. C. Higher-Accuracy Van Der Waals Density Functional. *Phys. Rev. B* **2010**, *82*, No. 081101.

(39) Murray, É. D.; Lee, K.; Langreth, D. C. Investigation of Exchange Energy Density Functional Accuracy for Interacting Molecules. *J. Chem. Theory Comput.* **2009**, *5*, 2754−2762.

(40) Heyd, J.; Scuseria, G. E.; Ernzerhof, M. Hybrid Functionals Based on A Screened Coulomb Potential. *J. Chem. Phys.* **2003**, *118*, 8207−8215.

(41) Chen, L.; Huan, T. D.; Quintero, Y. C.; Ramprasad, R. Charge Injection Barriers at Metal/Polyethylene Interfaces. *J. Mater. Sci.* **2016**, *51*, 506−512.

I